Content-Based Hyperspectral Image Retrieval Using Spectral Unmixing

Antonio J. Plaza[a]

[a]Hyperspectral Computing Laboratory
Department of Technology of Computers and Communications
University of Extremadura, Avda. de la Universidad s/n
10071 Cáceres, Spain

ABSTRACT

The purpose of content-based image retrieval (CBIR) is to retrieve, from real data stored in a database, information that is relevant to a query. A major challenge for the development of efficient CBIR systems in the context of hyperspectral remote sensing applications is how to deal with the extremely large volumes of data produced by current Earth-observing (EO) imaging spectrometers. The data resulting from EO campaigns often comprises many Gigabytes per flight. When multiple instruments or timelines are combined, this leads to the collection of massive amounts of data coming from heterogeneous sources, and these data sets need to be effectively stored, managed, shared and retrieved. Furthermore, the growth in size and number of hyperspectral data archives demands more sophisticated search capabilities to allow users to locate and reuse data acquired in the past. In this paper we develop a new strategy to effectively retrieve hyperspectral image data sets using spectral unmixing concepts. Spectral unmixing is a very important task for hyperspectral data exploitation since the spectral signatures collected in natural environments are invariably a mixture of the pure signatures of the various materials found within the spatial extent of the ground instantaneous field view of the imaging instrument. In this work, we use the information provided by spectral unmixing (i.e. the spectral endmembers and their corresponding abundances in the scene) as effective meta-data to develop a new CBIR system that can assist users in the task of efficiently searching hyperspectral image instances in large data repositories. The proposed approach is validated using a collection of 154 hyperspectral data sets (comprising seven full flightlines) gathered by NASA using the Airborne Visible Infra-Red Imaging Spectrometer (AVIRIS) over the World Trade Center (WTC) area in New York City during the last two weeks of September, 2001, only a few days after the terrorist attacks that collapsed the two main towers and other buildings in the WTC complex.

Keywords: Hyperspectral imaging, content-based image retrieval (CBIR), spectral unmixing, endmember extraction, abundance estimation.

1. INTRODUCTION

Content-based image retrieval (CBIR) intends to retrieve, from real data stored in a database, information that is relevant to a query.[1] This is particularly important in large data repositories, such as those available in remotely sensed hyperspectral imaging.[2] For instance, the NASA Jet Propulsion Laboratory's Airborne Visible Infra-Red Imaging Spectrometer (AVIRIS)[3] is able to record the visible and near infrared spectrum of the reflected light of an area several kilometers long (depending on the duration of the flight) using hundreds of spectral bands. The resulting 'image cube' is a stack of images (see Fig. 1), in which each pixel (vector) has an associated spectral signature or 'fingerprint' that uniquely characterizes the underlying objects. The resulting data often comprises several Gigabytes per flight.

One of the main problems involved in hyperspectral data exploitation is spectral unmixing,[4] as many of the pixels collected by imaging spectrometers such as AVIRIS are highly mixed in nature due to spatial resolution and other phenomena. For instance, it is very likely that the pixel labeled as 'vegetation' in Fig. 1 is actually composed of several types of vegetation canopies interacting at sub-pixel levels. The same comment applies to

Send correspondence to Antonio J. Plaza:
E-mail: aplaza@unex.es; Telephone: +34 927 257000 (Ext. 51662); URL: http://www.umbc.edu/rssipl/people/aplaza

Image and Signal Processing for Remote Sensing XVII, edited by Lorenzo Bruzzone,
Proc. of SPIE Vol. 8180, 81800O · © 2011 SPIE · CCC code: 0277-786X/11/$18 · doi: 10.1117/12.898833

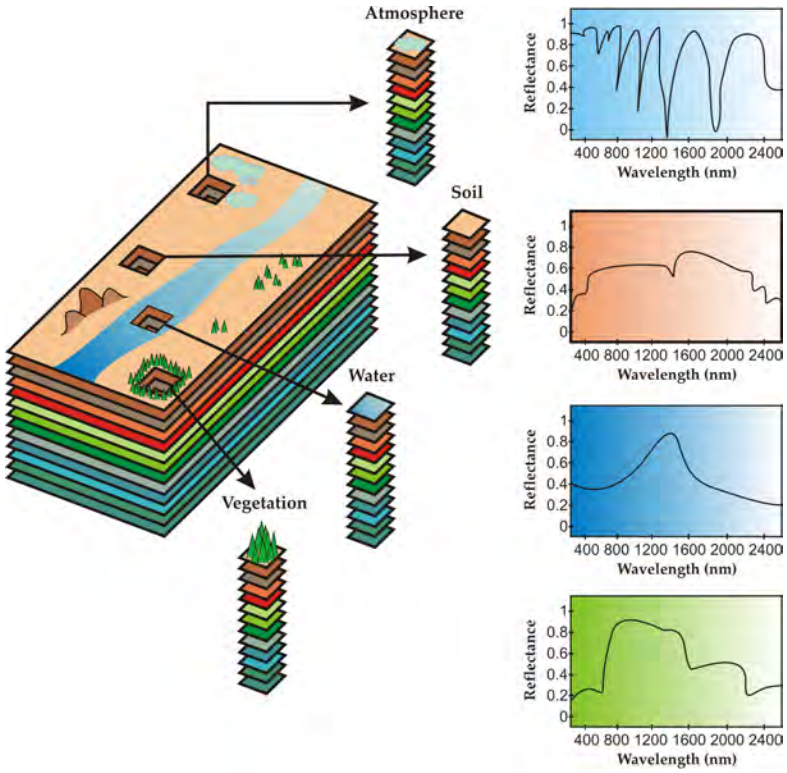

Figure 1. The concept of hyperspectral imaging.

the 'soil' pixel, which may comprise different types of geological features. As a result, spectral unmixing is a very important task for hyperspectral data exploitation since the spectral signatures collected in natural environments are invariably a mixture of the pure signatures of the various materials found within the spatial extent of the ground instantaneous field view of the imaging instrument. Among several techniques designed to deal with the inherent complexity of hyperspectral images in supervised fashion,[4,5] linear spectral unmixing follows an unsupervised approach which aims at inferring pure spectral signatures, called *endmembers*, and their material fractions, called *abundances*, at each pixel of the scene.

In this paper, we describe a new CBIR system for information extraction and mining from hyperspectral remote sensing data repositories which takes advantage of seminal concepts from linear spectral unmixing concepts[6] to perform effective data retrieval. Nowadays, it is estimated that a large fraction of collected hyperspectral data sets are never used but simply stored in a database, whereas these data already available in hyperspectral archives can be readily used in different application contexts or for different purposes than those that motivated the initial data collection, provided that effective CBIR mechanisms are in place to properly retrieve the data.[7] Here, we use the information provided by spectral unmixing (i.e. the spectral endmembers and their corresponding abundances in the scene) as effective meta-data to develop a new CBIR system that can assist users in the task of efficiently searching hyperspectral image instances in large data repositories.

The proposed innovative approach is experimentally validated using a collection of 154 hyperspectral data sets (comprising seven full flightlines) gathered by NASA using the Airborne Visible Infra-Red Imaging Spectrometer (AVIRIS) over the World Trade Center (WTC) area in New York City during the last two weeks of September, 2001, only a few days after the terrorist attacks that collapsed the two main towers and other buildings in the WTC complex. Our results indicate that the proposed system can efficiently retrieve hyperspectral images from a complex image database. The proposed system is expected to increase the value of the data acquired by airborne/satellite hyperspectral imaging instruments, and to improve the end-user services available in hyperspectral image databases. The remainder of the paper is structured as follows. Section 2 describes the considered spectral unmixing methodology used to implement the core of our CBIR system. Section 3 describes

the proposed CBIR system. Section 4 assesses the performance of the system by comparing its retrieval accuracy using a large database of AVIRIS images. Section 5 concludes with some remarks and future research avenues.

2. SPECTRAL UNMIXING METHODOLOGY

Let us assume that a remotely sensed hyperspectral image with n bands is denoted by $\mathbf{I}$, in which a pixel of the scene is represented by a vector $\mathbf{x} = [x_1, x_2, \cdots, x_n] \in \Re^N$, where $\Re$ denotes the set of real numbers in which the pixel's spectral response x_k at sensor channels $k = 1, \ldots, n$ is included. Under the linear mixture model assumption,[8,9] each pixel vector in the original scene can be modeled using the following expression:

$$\mathbf{x} \approx \mathbf{E}\mathbf{a} + \mathbf{n} = \sum_{i=1}^{p} \mathbf{e}_i a_i + \mathbf{n}, \tag{1}$$

where $\mathbf{E} = \{\mathbf{e}_i\}_{i=1}^{p}$ is a matrix containing p pure spectral signatures (endmembers), $\mathbf{a} = [a_1, a_2, \cdots, a_p]$ is a p-dimensional vector containing the abundance fractions for each of the p endmembers in $\mathbf{x}$, and $\mathbf{n}$ is a noise term. Solving the linear mixture model involves: 1) identifying a collection of $\{\mathbf{e}_i\}_{i=1}^{p}$ endmembers in the image, and 2) estimating their abundance in each pixel $\mathbf{x}$ of the scene. These processing steps can be summarized as follows:

2.1 Endmember extraction

Firstly, a set of $\mathbf{E} = \{\mathbf{e}_i\}_{i=1}^{p}$ endmember signatures are extracted from the input data set. For this purpose we consider the N-FINDR algorithm,[10] one of the most widely used and successfully applied methods for automatically determining endmembers in hyperspectral image data without using a priori information. This algorithm looks for the set of pixels with the largest possible volume by *inflating* a simplex inside the data. The procedure begins with a random initial selection of pixels. Every pixel in the image must be evaluated in order to refine the estimate of endmembers, looking for the set of pixels that maximizes the volume of the simplex defined by selected endmembers. The corresponding volume is calculated for every pixel in each endmember position by replacing that endmember and finding the resulting volume. If the replacement results in a an increase of volume, the pixel replaces the endmember. This procedure is repeated in iterative fashion until there are no more endmember replacements. The method can be summarized by a step-by-step algorithmic description which is given below for clarity:

1. *Feature reduction.* Apply a dimensionality reduction transformation such as the principal component analysis (PCA)[11] to reduce the dimensionality of the data from n to $p-1$, where p is an input parameter to the algorithm (number of endmembers to be extracted).

2. *Initialization.* Let $\{\mathbf{e}_1^{(0)}, \mathbf{e}_2^{(0)}, \cdots, \mathbf{e}_p^{(0)}\}$ be a set of endmembers randomly extracted from the input data.

3. *Volume calculation.* At iteration $k \geq 0$, calculate the volume defined by the current set of endmembers as follows:
$$V(\mathbf{e}_1^{(k)}, \mathbf{e}_2^{(k)}, \cdots, \mathbf{e}_p^{(k)}) = \frac{\left|\det \begin{bmatrix} 1 & 1 & \cdots & 1 \\ \mathbf{e}_1^{(k)} & \mathbf{e}_2^{(k)} & \cdots & \mathbf{e}_p^{(k)} \end{bmatrix}\right|}{(p-1)!}. \tag{2}$$

4. *Replacement.* For each pixel vector $\mathbf{x}$ in the input hyperspectral data, recalculate the volume by testing the pixel in all p endmember positions, i.e., first calculate $V(\mathbf{x}, \mathbf{e}_2^{(k)}, \cdots, \mathbf{e}_p^{(k)})$, then calculate $V(\mathbf{e}_1^{(k)}, \mathbf{x}, \cdots, \mathbf{e}_p^{(k)})$, and so on until $V(\mathbf{e}_1^{(k)}, \mathbf{e}_2^{(k)}, \cdots, \mathbf{x})$. If none of the p recalculated volumes is greater than $V(\mathbf{e}_1^{(k)}, \mathbf{e}_2^{(k)}, \cdots, \mathbf{e}_p^{(k)})$, then no endmember is replaced. Otherwise, the combination with maximum volume is retained. Let us assume that the endmember absent in the combination resulting in the maximum volume is denoted by $\mathbf{e}_i^{(k+1)}$. In this case, a new set of endmembers is produced by letting $\mathbf{e}_i^{(k+1)} = \mathbf{x}$ and $\mathbf{e}_l^{(k+1)} = \mathbf{e}_l^{(k)}$ for $l \neq i$. The replacement step is repeated for all the pixel vectors in the input data until all the pixels have been exhausted.

2.2 Abundance estimation

Once the set of endmembers $\mathbf{E} = \{\mathbf{e}_i\}_{i=1}^{p}$ have been extracted, an unconstrained solution to (1) is simply given by the following expression:[2]

$$\mathbf{a} \approx (\mathbf{E}^T\mathbf{E})^{-1}\mathbf{E}^T\mathbf{x}. \tag{3}$$

However, two physical constrains are generally imposed in order to estimate the p-dimensional vector of abundance fractions $\mathbf{a} = [a_1, a_2, \cdots, a_p]$ at a given pixel $\mathbf{x}$, these are the abundance non-negativity constraint (ANC), i.e., $a_i \geq 0$ for all $1 \leq i \leq p$, and the abundance sum-to-one constraint (ASC), i.e., $\sum_{i=1}^{p} a_i = 1$.[9] Imposing the ASC constraint results in the following optimization problem:

$$\min_{\mathbf{a}\in\Delta} \left\{ (\mathbf{x} - \mathbf{a}\cdot\mathbf{E})^T (\mathbf{x} - \mathbf{a}\cdot\mathbf{E}) \right\}, \text{ subject to: } \Delta = \left\{ \mathbf{a} \,\middle|\, \sum_{i=1}^{p} a_i = 1 \right\}. \tag{4}$$

Similarly, imposing the ANC constraint results in the following optimization problem:

$$\min_{\mathbf{a}\in\Delta} \left\{ (\mathbf{x} - \mathbf{a}\cdot\mathbf{E})^T (\mathbf{x} - \mathbf{a}\cdot\mathbf{E}) \right\}, \text{ subject to: } \Delta = \{\mathbf{a} | a_i \geq 0 \text{ for all } 1 \leq a \leq p\}. \tag{5}$$

As indicated in,[9] a fully constrained (i.e. ASC-constrained and ANC-constrained) estimate can be obtained in least-squares sense by solving the optimization problems in (4) and (5) simultaneously. Such fully constrained linear spectral unmixing estimate is generally referred to in the literature by the acronym FCLSU.[9]

3. PROPOSED CBIR SYSTEM

The proposed CBIR system for retrieval of hyperspectral imagery is based on the spectral unmixing methodology described in the previous section. In this section, we describe the stages involved in a standard search procedure using the proposed CBIR system from an user's point of view:

1. *Input query*. The user first selects a portion or a full hyperspectral scene to be used as an input image image $\mathbf{I}$. Then, the system computes a feature vector associated to that portion given by the spectral signatures of endmembers $\mathbf{E} = \{\mathbf{e}_i\}_{i=1}^{p}$, derived using the N-FINDR algorithm, and their correspondent FCLSU-derived abundances summed across all the pixels in the considered portion. The number of endmembers to be extracted from the sample portion is automatically calculated using the hyperspectral signal identification by minimum error (HySime) method.[12]

2. *Signature comparison and sorting*. The feature vector obtained in the previous stage, which comprises the p endmembers and their macroscopical abundances in the selected image portion $\mathbf{I}$, is stored in a header file associated to $\mathbf{I}$ and compared with the pre-computed feature vectors of all the hyperspectral images in the database, using the following spectral signature matching algorithm (SSMA). Let $\{\mathbf{e}_i\}_{i=1}^{p}$ be a set of p endmembers extracted from the considered image $\mathbf{I}$, and let $\{\mathbf{r}_j\}_{j=1}^{q}$ be a set of q endmembers extracted from a reference hyperspectral image $\mathbf{R}$ already available in the database (we assume that the database contains a large number of hyperspectral images). The idea now is to analyze if $\mathbf{R}$ should be retrieved as a hyperspectral image that is 'sufficiently similar' with regards to $\mathbf{I}$. It should be noted that the endmembers and their corresponding abundances are stored for each image data set catalogued in the system as part of the image header file, hence we use this information in order to decide about the similarity of the compared images. To accomplish this task, we use a spectral angle distance (SAD)-based[8] similarity criterion which is implemented using the following steps:

   (a) *Initial labeling*. Label all endmembers in the test set $\{\mathbf{e}_i\}_{i=1}^{p}$ as 'unmatched.'

   (b) *Matching*. For each unmatched endmember in the test set $\{\mathbf{e}_i\}_{i=1}^{p}$, calculate the spectral angle between the test endmember and all endmembers in the reference set $\{\mathbf{r}_j\}_{j=1}^{q}$. If the pair $(\mathbf{e}_k, \mathbf{r}_l)$, with $1 \leq k \leq p$ and $1 \leq l \leq q$, results in the minimum obtained value of $\text{SAD}(\mathbf{e}_k, \mathbf{r}_l)$, and the value is below threshold angle v_a, then label the associated endmembers, $\mathbf{e}_k$ and $\mathbf{r}_l$ as 'matched.'

Figure 2. AVIRIS hyperspectral image collected over the World Trade Center (left) and detail of the area used as input query (right).

(c) *Relative difference calculation.* For each matched endmember $\mathbf{e}_k$ resulting from the previous step, calculate the relative difference between the abundance fraction associated to endmember $\mathbf{e}_k$ in the test image and the abundance associated to its matched endmember $\mathbf{r}_l$ in the reference image. The resulting values are used as a feature vector for signature comparison when searching the database. After this process, the identifiers of the M images which are most similar to the test image are extracted and ranked in descending order of similarity.

3. *Display of results*. A mosaic made up of the first M images selected is assembled and then presented to the user as the search result.

4. *Query update*. If the user considers the search result to be unsatisfactory, he may select one of the displayed images (or a different portion of the original image) as a new input, and then return to the first stage. The system keeps track of successful and unsuccessful queries as identified by the user.

4. EXPERIMENTAL RESULTS

In order to illustrate the performance of our unmixing-based CBIR system, we specifically address a case study of urban monitoring and assessment, using a collection of 154 high-resolution hyperspectral data sets (comprising a total space of more than 20 Terabytes) gathered by NASA over the World Trade Center (WTC) area in New York City during the last two weeks of September, 2001, just several days after the terrorist attacks that collapsed the two main towers and other buildings in the WTC complex. In all cases, the spatial resolution is of 3.7 meters per pixel, and the spectral resolution is of 224 narrow spectral bands between 0.4 and 2.5 micrometers. Fig. 2 shows a false color composite of one of such images, with 614×512 pixels and 224 bands. The false color composition has been formed using the 1682, 1107 and 655 nm channels, displayed as red, green and blue, respectively. Vegetated areas appear green in Fig. 2, while burned areas appear dark gray. Smoke coming from the WTC area appears bright blue due to high spectral reflectance in the 655 nm channel. The area used as input query in our experiment is shown in a red rectangle, and is centered at the region where the towers collapsed. This area contains spectral signatures of thermal hot spots corresponding to fires in the area. The fact that our search area contains such spectral signatures was expected to assist in the detection of other images containing fires across the entire database, which is an useful task in order to assist in the detection of such fires at sub-pixel levels, thus contributing to the extinction efforts conducted in the area.

Using the search area in the rightmost part of Fig. 2 as input query, the proposed parallel CBIR system successfully retrieved all image instances ($M = 7$) containing the WTC complex across the database, with no

false positive detections. The threshold angle value used to implement the SAD-based similarity criterion of SSMA was set to $v_a = 0.1$, a reasonable limit of tolerance for this metric as described before in the literature.[13]

For illustrative purposes, Fig. 3 shows the seven full image flightlines in the considered AVIRIS database that contain the searched area centered at the WTC complex. On the other hand, Fig. 4 shows some of the full image flightlines in the considered database that do not contained the searched area. Typically, each flightline comprises from 5 to 7 individual images, and a total of 24 full flightlines were considered in our experiments*. As shown by Figs. 3 and 4, the complexity of the scenes is very high due to smoke and urban interferers in the scene which difficult the identification of areas with hot spot thermal fires, which are used as a search criterion in this experiment. In this regard, the proposed CBIR system performed very accurately in this task, thus serving as a relevant tool for content-based retrieval of hyperspectral images based on a complex search criterion: the presence of fires, which in many cases can only be detected a sub-pixel levels.

In addition, the signature comparison and sorting times achieved by queries in the proposed CBIR algorithm were very low as only the information in the header files (p endmembers and their summed abundances across the scene) are involved in the calculations. Hence, we can conclude that the most time consuming part of the system is the time to catalog a new image entry, which amounts to finding the p endmembers associated to the image and their FCLSU-derived abundances. Recently, we have demonstrated that this task can be accomplished in real-time (i.e., in a time lower to the one invested by the AVIRIS sensor in collecting the data) using different high performance computing platforms such as multi-core processors,[14] clusters of computers,[7,15] heterogeneous networks of workstations,[16] or commodity graphics processing units,[17] hence the proposed system can be implemented efficiently to achieve fast performance. An operational system for distributed platforms similar to the one presented in[18] but using the proposed CBIR technology is already available.[16] This leads to the appealing possibility of rapidly providing emergency response teams with information on the presence of fires and the evolution in the distribution of debris and other materials in the dusts deposited around the WTC area in this particular case study.

5. CONCLUSIONS AND FUTURE RESEARCH

In this paper, we have developed an innovative CBIR system for hyperspectral image retrieval based on spectral unmixing concepts. The proposed system first extracts the spectral endmembers and then uses them (together with their relative abundance fractions) as a feature vector to perform a database query based on sub-pixel image content. The system has been implemented using well-known algorithms in the spectral unmixing community, such as the HySime for estimating the number of endmembers in a given scene, the N-FINDR algorithm for extracting the spectral signatures of such endmembers, and the FCLSU algorithm for fully-constrained abundance estimation of the endmembers in a given scene. Our experimental results, conducted using a large database made up of 154 hyperspectral scenes collected by the AVIRIS instrument over the World Trace Center in New York, five days after the terrorist attacks, indicate that the proposed CBIR system can accurately extract hyperspectral image instances from a complex image database with sub-pixel precision and quickly enough for practical use. This can be accomplished by resorting to available parallel implementations of the considered spectral unmixing chain in different types of high performance computing architectures. As a result, we believe that the proposed system can adequately exploit the source of computational power currently offered by such architectures, thus making the proposed tool accessible and applicable to obtaining results quickly enough and with high reliability in many on-going and planned Earth-observing missions. As a future extension of the system, we plan to develop a distributed database implementation that may provide competitive advantages in terms of increased availability, quality of service, and ease of expansion. We also intend to include other forms of spectral unmixing in the proposed system, possibly exploiting different types of ancillary data potentially available *a priori*, including any form of reference data with the potential to assist in a better characterization of nonlinear mixtures.

ACKNOWLEDGEMENT

This work has been supported by the European Community's Marie Curie Research Training Networks Programme under reference MRTN-CT-2006-035927 (HYPER-I-NET). Funding from the Spanish Ministry of Science and Innovation (HYPERCOMP/EODIX project, reference AYA2008-05965-C04-02) is gratefully acknowledged.

*See http://aviris.jpl.nasa.gov/ql/listg01.html

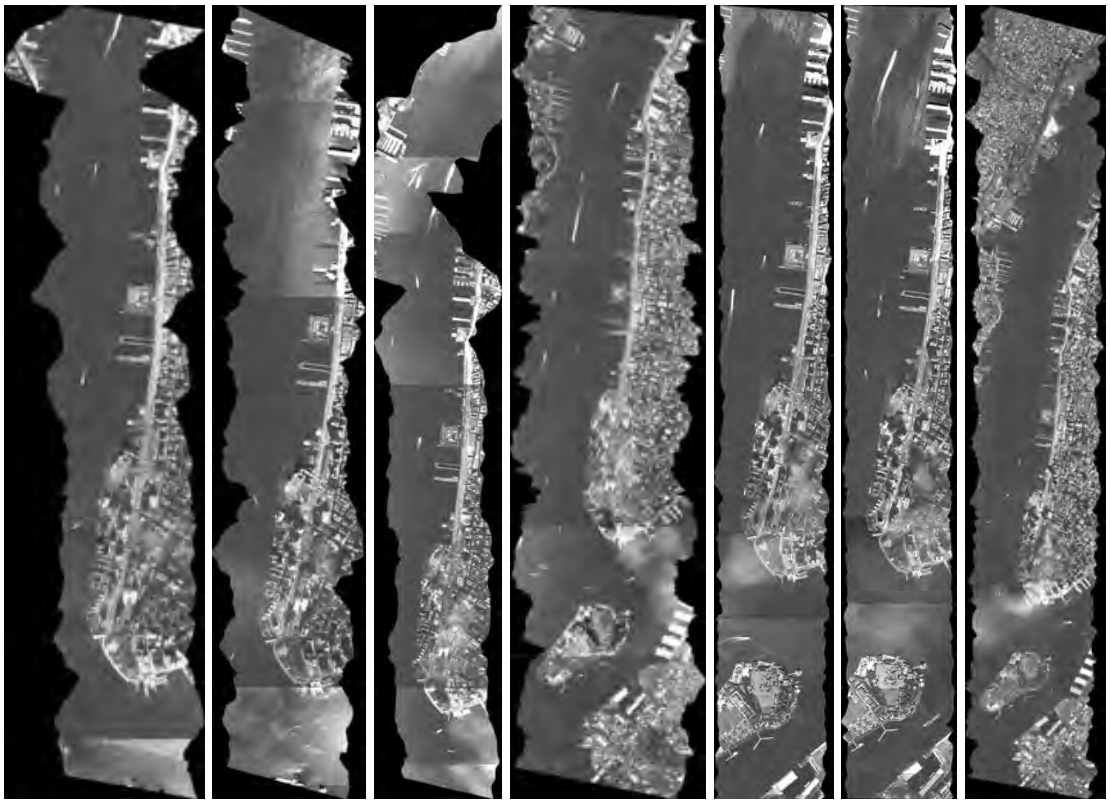

Figure 3. Full flightlines collected by the AVIRIS sensor over the World Trade Center area which contain the search area in Fig. 2. Typically, each flightline contains 5 to 7 hyperspectral images (each with 224 spectral bands).

REFERENCES

1. A. W. M. Smeulders, M. Worring, S. Santini, A. Gupta, and R. Jain, "Fast dimensionality reduction and simple PCA," *IEEE Transactions on Pattern Analysis and Machine Intelligence* **22**, pp. 1349–1380, 2000.
2. C.-I. Chang, *Hyperspectral Imaging: Techniques for Spectral Detection and Classification*, Kluwer Academic/Plenum Publishers: New York, 2003.
3. R. O. Green, M. L. Eastwood, C. M. Sarture, T. G. Chrien, M. Aronsson, B. J. Chippendale, J. A. Faust, B. E. Pavri, C. J. Chovit, M. Solis, *et al.*, "Imaging spectroscopy and the airborne visible/infrared imaging spectrometer (AVIRIS)," *Remote Sensing of Environment* **65**(3), pp. 227–248, 1998.
4. A. Plaza, J. A. Benediktsson, J. Boardman, J. Brazile, L. Bruzzone, G. Camps-Valls, J. Chanussot, M. Fauvel, P. Gamba, J. Gualtieri, M. Marconcini, J. C. Tilton, and G. Trianni, "Recent advances in techniques for hyperspectral image processing," *Remote Sensing of Environment* **113**, pp. 110–122, 2009.
5. G. Camps-Valls and L. Bruzzone, "Kernel-based methods for hyperspectral image classification," *IEEE Transactions on Geoscience and Remote Sensing* **43**, pp. 1351–1362, 2005.
6. J. B. Adams, M. O. Smith, and P. E. Johnson, "Spectral mixture modeling: a new analysis of rock and soil types at the Viking Lander 1 site," *Journal of Geophysical Research* **91**, pp. 8098–8112, 1986.
7. A. Plaza, J. Plaza, A. Paz, and S. Sanchez, "Parallel hyperspectral image and signal processing," *IEEE Signal Processing Magazine* **28**(3), pp. 119–126, 2011.
8. N. Keshava and J. F. Mustard, "Spectral unmixing," *IEEE Signal Processing Magazine* **19**(1), pp. 44–57, 2002.
9. D. Heinz and C.-I. Chang, "Fully constrained least squares linear mixture analysis for material quantification in hyperspectral imagery," *IEEE Transactions on Geoscience and Remote Sensing* **39**, pp. 529–545, 2001.
10. M. E. Winter, "N-FINDR: An algorithm for fast autonomous spectral endmember determination in hyperspectral data," *Proceedings of SPIE* **3753**, pp. 266–277, 1999.

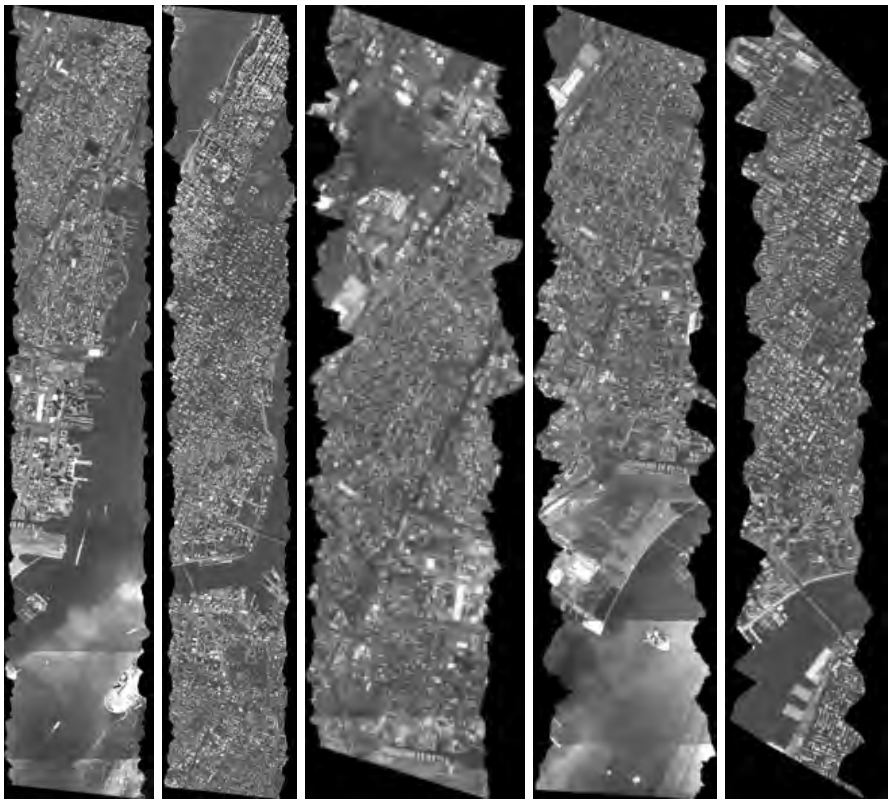

Figure 4. Full flightlines collected by the AVIRIS sensor over the World Trade Center area which do not contain the search area in Fig. 2. Typically, each flightline contains 5 to 7 hyperspectral images (each with 224 spectral bands).

11. J. A. Richards and X. Jia, *Remote Sensing Digital Image Analysis: An Introduction*, Springer, 2006.
12. J. M. Bioucas-Dias and J. M. P. Nascimento, "Hyperspectral subspace identification," *IEEE Trans. Geosci. Remote Sens.* **46**(8), pp. 2435–2445, 2008.
13. A. Plaza, P. Martinez, R. Perez, and J. Plaza, "A quantitative and comparative analysis of endmember extraction algorithms from hyperspectral data," *IEEE Transactions on Geoscience and Remote Sensing* **42**(3), pp. 650–663, 2004.
14. A. Remon, S. Sanchez, A. Paz, E. S. Quintana-Orti, and A. Plaza, "Real-time endmember extraction on multi-core processors," *IEEE Geoscience and Remote Sensing Letters* **8**, pp. 924–928, 2001.
15. A. Plaza, Q. Du, Y.-L-Chang, and R. L. King, "High performance computing for hyperspectral remote sensing," *IEEE Journal of Selected Topics in Applied Earth Observations and Remote Sensing* **4**(3), 2011.
16. A. Plaza, J. Plaza, and A. Paz, "Content-based image retrieval at the end of the early years," *Concurrency and Computation: Practice and Experience* **9**, pp. 1138–1159, 2010.
17. S. Sanchez, A. Paz, G. Martin, and A. Plaza, "Parallel unmixing of remotely sensed hyperspectral images on commodity graphics processing units," *Concurrency and Computation: Practice and Experience* **23**(12), 2011.
18. D. Brunner, G. Lemoine, F.-X. Thoorens, and L. Bruzzone, "Distributed geospatial data processing functionality to support collaborative and rapid emergency response," *IEEE Journal of Selected Topics in Applied Earth Observations and Remote Sensing* **2**(1), pp. 33–46, 2009.